Sheet Atomization of Gel Propellant Simulant

K. Vivek, Aditya Saurabh, Devendra Deshmukh, Deepak Agarwal, and Lipika Kabiraj

Abstract Gelled propellants for rocket propulsion applications offer the advantage of safer storage and handling in comparison with liquid fuels. Sheet formation and break-up study of non-reactive gel simulant prepared with Carbopol 934 in de-ionized water was conducted for understanding atomization of gels by impinging jets configuration. Material properties of gels prepared and their flow behavior estimated. The simulant is injected through an orifice of 0.413 mm up to a range of 20 bar injection pressure is studied by analyzing high-speed shadow graph images of liquid jets impingement, sheet formation, and disintegration. The prominent effect of gelling agent concentration in sheet formation and break-up is revealed. Sheet break-up is occurring in two different modes for five different gel concentrations. Waves generated from impingement point caused break-up of sheets for low-concentration gels and high-velocity jets while tearing and hole formation in sheets led to their break-up for mostly high-concentration gels and particularly for low jet velocity modes. Droplet trajectories and their velocity at various locations in the periphery of sheets were measured for two different jet velocities for five gel concentrations.

Keywords Gel propellants · Atomization · Non-Newtonian

K. Vivek (✉) · L. Kabiraj
Indian Institute of Technology Ropar, Ropar, Punjab 140001, India
e-mail: 2018mez0025@iitrpr.ac.in

L. Kabiraj
e-mail: lipika.kabiraj@iitrpr.ac.in

A. Saurabh
Indian Institute of Technology Kanpur, Kanpur 208016, India
e-mail: asaurabh@iitk.ac.in

D. Deshmukh
Indian Institute of Technology Indore, Indore, Madhya Pradesh 453552, India
e-mail: dldeshmukh@iiti.ac.in

D. Agarwal
Indian Space Research Organization, Valiamala, Kerala 695547, India

1 Introduction

In rocket propulsion, the requirement of energy dense and safe to operate fuel is of utmost importance. Gelled propellants offer these two essential qualities and qualify for further study of their atomization and combustion characteristics. The non-Newtonian nature of gelled propellants, along with yield stress, allows its storage like solid materials for which safety issues like leakage, sloshing, and spilling are non-existent. Having addressed these issues takes these gel propellants to the next level of requirement of a fuel which is the atomization capability. Fuel drop size and its distribution are a big concern for liquid fuels. High viscosity and shear thinning behaviors play advantage and disadvantage from the atomization angle. The impinging fluid jet configuration has better oxidizer fuel mixing and atomization capabilities. The liquid disintegration process depends on liquid injection pressure, injector design, and liquid properties. The studies include sheet dimensions like break-up length, sheet width, droplet formation sites, droplet velocity distribution, droplet size, and distributions. Liquid propellants are Newtonian, whereas, gelled propellants are non-Newtonian. Water is a simulant for propellant simulant as its physical properties are similar. Preparation of gelled propellant simulants involves a simulant for the propellant and a gelling agent which will dissolve in the propellant simulant.

Various reports about studies on the impinging jet of Newtonian liquids are fundamental steps for the non-Newtonian liquids. Reference [1] reported four different spray regimes for three different fluids with different physical properties. These regimes were closed rim pattern, periodic drop regime, sheet rim separation, and fully developed regime within a jet velocity range of 1.5–30.5 ms^{-1}. Sheet width and sheet length increase as jet velocity increased and reach a maximum value before fully developed flow. Hydrodynamic waves were observed above a critical liquid jet Weber number. Reference [2] study on impinging jet up to a jet velocity of 25 ms^{-1} found that sheet break-up length increases with velocity and decrease of impingement angle. Theoretical study of two cylindrical impinging jets of fluid by [3] showed two break-up regimes. A low Weber number regime sheet dimensions were similar to experimentally measured values reported earlier, and the break-up is due to Taylor cardioidal waves, and a high Weber number break-up regime where break-up was due to Kelvin–Helmholtz instability. A study by [4] on Newtonian fluids with an impingement angle of 90° using 0.5 mm diameter injector showed ten different spray patterns, mostly subcategories found by [1]. For different surface tension and viscosity fluids, the sheet formed by impinging jets had a constant sheet length to width ratio for an increase in jet velocity, and this ratio increased with an increase in jet velocity.

Carbopol 941 in water described as power law fluid was used [5] to simulate RP-1 gelled fuel and water as RP-1 and reported low atomization quality because of high viscosity [6]. Carbopol 941 gel was also used as a simulant. A low break-up tendency of liquid was observed, which was attributed to higher intermolecular forces within the gel. Gelled kerosene loaded with Al particles and was atomized [7]

by impinging liquid jets from an injector of orifice 1.5 mm for a jet velocity range of 10–20 ms^{-1}. High shear rates induced in the gel while flowing and impingement reduced the viscosity and mean droplet diameter. Ostwald and HB models were found suitable to describe the rheological behavior of Carbopol gels [8]. In [9], the HB model explained metalized gelled jet A1 fuel and observed a reduction in viscosity for increased shear rates. They identified three different spray patterns: ray shaped, ligament pattern, and a fully developed pattern for low, medium, and high generalized Reynolds number (Eq. 1). Various Newtonian liquids were studied [10] with an impinging jet configuration using 1 mm orifice injector. Regimes, namely ray shaped structure, rim and droplet separation, rimless separation, ligament structure, and fully developed patterns, are identified under a Reynolds Number and Weber number plot [11]. Study on Carbopol 941 was conducted with a triplet impinging set up with an orifice diameter of 1.1 mm.

They observed a delay in liquid break-up and atomization and explained that it was due to the gel's higher viscosity. Spray patterns with rims are also identified. Comparison [12] of sheet formation and disintegration of gelled and non-gelled water reported lesser disturbances in the sheet due to higher viscosity. For an increase in Reynolds number, break-up length was found to decrease. Carbopol 934 gel loaded with SUS302 nanoparticles was used [13] to study the rheological characteristics. Shear-thinning nature and presence of yield stress was reported, and the gel was described as HB fluid. The extended HB model was used to explain paraffin, jet A-1, and ethanol-based gelled fuels [14]. This extended model was mentioned to take consideration of whole range of shear rates occurring in propulsion application. Carbopol 934 gel atomization by impinging jets was compared with that of water [15]. The sheet length was found to increase with an increase in jet velocity. Four types of spray patterns were identified: open rim and no shedding drop; rimless sheet with ray shaped shedding; sheet with ligament separation; fully developed. Mean droplet diameter was also decreasing with an increase in jet velocity and converged to an asymptotic number. Carbopol gel was studied [16] and saw that the linear stability analysis method yield similar results to that of experimental for sheet break-up length and wavelength of power-law sheets. The break-up length and wavelength were found to decrease with an increase in Weber number. An impinging jet study [17] with Carbopol 934 solution using 0.6 mm orifice injectors and showed the existence of six types of spray pattern; open rim without shedding droplet, closed rim, open rim with shedding droplet, rimless sheet, bow-shaped ligament, and fully developed. The flow behavior under shear was described using power law. They also measured droplet velocities across various axes and observed higher velocities for larger droplets. The impact wave regime of impinging jets of gelled rocket propellant ISROsene loaded with alumina particles and had the wave propagation velocity to be slower than that of jets [18]. Break-up length increased with Weber number. An SMD of 200–400 μm was also observed [19]. In sheet formation of gel propellant, two new regimes were discovered, open rim with holes, and impact wave with longitudinal ligaments. Uneven distribution of mass or clustering of particles was seen as the reason for these regimes.

With this information, a detailed study on Carbopol 934 gel's atomization is conducted on a doublet like on like impinging jet configuration. Liquid sheet break-up, droplet velocity, and trajectory for different gelling agent concentrations under a range of injection pressures are studied.

2   Experiments and Setup

Carbopol 934 is an acrylic acid polymer soluble in water. Gel simulants are prepared using this gelling agent. A measured amount of gelling agent is mixed with de-ionized water (18.2 MΩ) by continuous stirring at 800 rpm using a magnetic stirrer. Stirring is continued up to twelve hours for proper dilution of the gelling agent. The pH of the solution is maintained neutral by the addition of Triethanolamine (TEA). The addition of TEA will produce a clear gel. After preparation of gel, it is stored in an airtight container. Gel samples with Carbopol concentration varying from 0.10 to 0.35 wt% by weight were prepared and stored. The surface tension of these samples was measured by pendant drop test in FTA1000 series contact angle instrument by First Ten Angstrom. This instrument uses the Laplace-Young equation to calculate surface tension. Variation of viscosity with the shear rate for each gel concentration is studied by rotational rheometer. Parallel plate geometry with 50 mm diameter flat plates and a gap of 1 mm between the plates is set for all measurements. A constant pre-shear of 10 s^{-1} is given for 100 s to the sample to remove any shear history. An idle time of another 100 s will ensure the reversal of all stress. The sample is made to undergo a rotational shear rate test with shear rates increasing logarithmically from 0.001 to 1000 s^{-1} in a duration of 3000 s.

A view of schematic diagram for spray characterization of two impinging jets in like on like configuration is shown in Fig. 1. Liquid fuel is stored in a 70 mm bore stainless steel cylinder. Pressurized nitrogen gas displaces an aluminum piston inside the cylinder for a maximum length of 300 mm. This piston drives out the liquid from the cylinder through two polyurethane tubes of 9 mm inner diameter whose other ends are connected to two nozzles of 0.41 mm. The impingement angle and pre-impingement length can be varied, and for the study, 2θ was kept at 900, and the pre-impingement length was 10 mm. An ultrasonic sensor tracked the movement of piston. Pressure transducers mounted at reservoir exit. A valve connected at the end of the cylinder restricts the flow of fluid. The fluid coming out through the orifices is collected in a vessel which is kept below the impingement location, and one nozzle entrance shows corresponding pressure values.
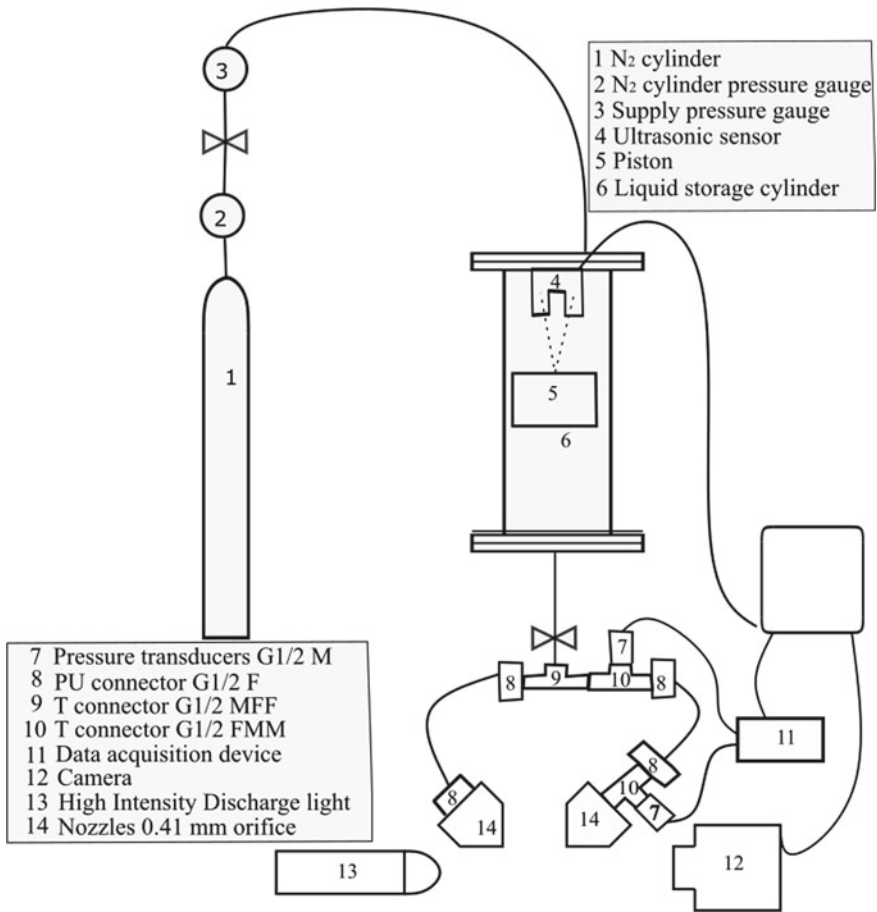
Fig. 1 Schematic diagram of atomization equipment and image acquisition

3 Experiments and Setup

3.1 Rheology Measurements

Results from rheology measurements of gel concentrations (0.10–0.35 wt%) confirmed the fluid's shear-thinning nature. Test up to a shear rate of 1000 s^{-1} showed that viscosity is continuously decreasing with an increase in shear rate. Figure 2 shows the viscosity-shear rate trends for gel concentrations on a log scale. As the concentration of the gelling agent increases, the viscosity is also found to be increasing. Kim et al. (2003) observed that more gelling agents increase the network structure inside the gel, thus requiring more shear stress to break the structures and
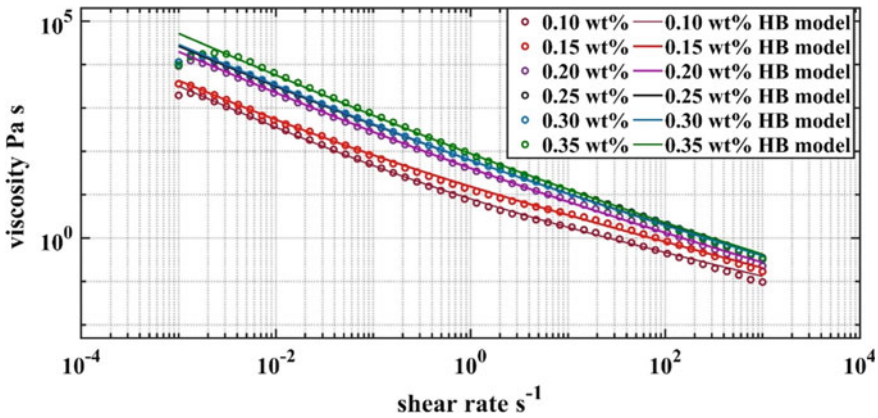
Fig. 2 Viscosity-shear rate trend and corresponding HB fluid model fit

flow. Herschel–Bulkley model is fitted to the experimental data point, and parameters describing the HB model are obtained. The model is given in Eq. 2.

$$\mu = \frac{\tau_0}{\dot\gamma} + K\dot\gamma^{n-1}. \tag{1}$$

The presence of yield stress was noted for all gel concentrations tested. The value of yield stress increased with an increase in gel concentration. For 0.10 wt% gel, the yield stress is 3 Pa, which is very low, and for 0.35 wt% the value for yield stress is found to be 48 Pa. This shows that as gel concentration increases, the gel behaves more like solid and more amount of initial stress is required to overcome the yield stress and make the gel start flowing. In Fig. 2, when the shear rate reached the maximum value, all the cases viscosity dropped below 1 Pa s. It is expected that a further increase in shear rate will take the viscosity value to a much lower level compared to that of water, which is the base fluid of the Carbopol gel. As gel travels through the nozzle and impinges, a high shear rate is expected to occur, which will reduce viscosity and thus atomization of the gel. As gel concentration increases, the exponent index, n, is decreasing. This shows that the liquid viscosity is getting more sensitive to change in shear rates. The HB model fit parameters are presented in Table 1. The density of the gel concentrations is taken to be 1000 kg m^{-3} and all measurements are carried out at a temperature of 25 °C.

3.2 Jet Velocity

The graphical relation between injection pressure and jet velocity of fluids studied is shown in Fig. 3. It is clear from the figure that the initial injection pressure required to

Table 1 HB model parameters for gel concentrations

Carbopol (wt%)	Yield stress (Pa)	Consistency factor (Pa s^n)	Exponent index
0.10	3.001	5.01	0.47
0.15	3.571	11.83	0.41
0.20	17.82	22.82	0.35
0.25	22.63	39.3	0.32
0.30	25.25	37.11	0.33
0.35	48	40.25	0.32
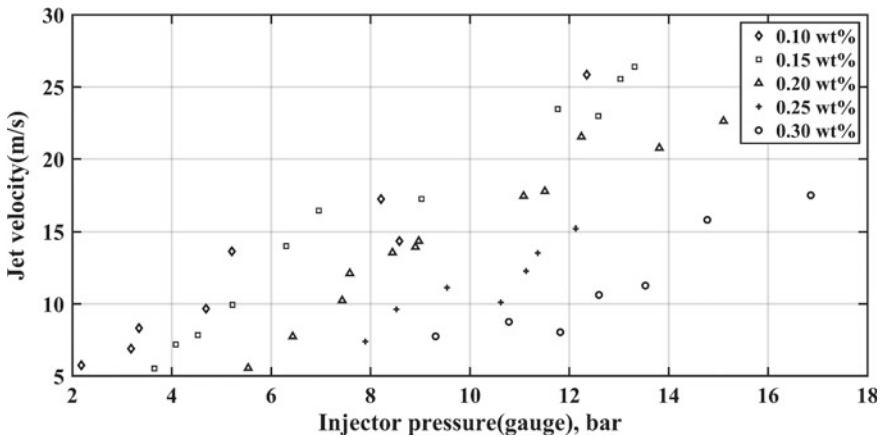
**Fig. 3** Injection pressure versus jet velocity for five gel concentrations

make the liquid flow through the orifice increases for an increase in gallant concentration. For a concentration above 0.10 wt%, the existence of yield stress is shown. The shear-thinning nature of gels prepared and the existence of yield stress confirms the excellent selection of fluid model selected for this work. The increase in yield stress is due to the increased quantity of gelling agents which creates more network-like structures in the fluid. To break the firm structures, initial stress is required. After breaking the bonds, the liquid starts to flow. Measurements conducted were for low jet velocity range, 5–30 ms^{-1}.

$$\text{Regen} = \frac{\rho v^{2-n} d_0^n}{K \left(\frac{3n+1}{4n}\right)^n 8^{n-1}} \qquad (2)$$

As the gels under study are non-Newtonian power-law fluids, a non-dimensional form of flow can be represented by generalized Reynolds number as shown in Eq. (2).

3.3 Sheet Break-up

Figure 4 shows representative images of spray formed by impinging jets of all gel concentrations at various injection pressures, with each row representing one gel concentration and five distinct injection pressure conditions starting from 0.10 wt% gel and ending with 0.30 wt% gel. The impinging jets form liquid sheets on a plane perpendicular to the axis of liquid jets.
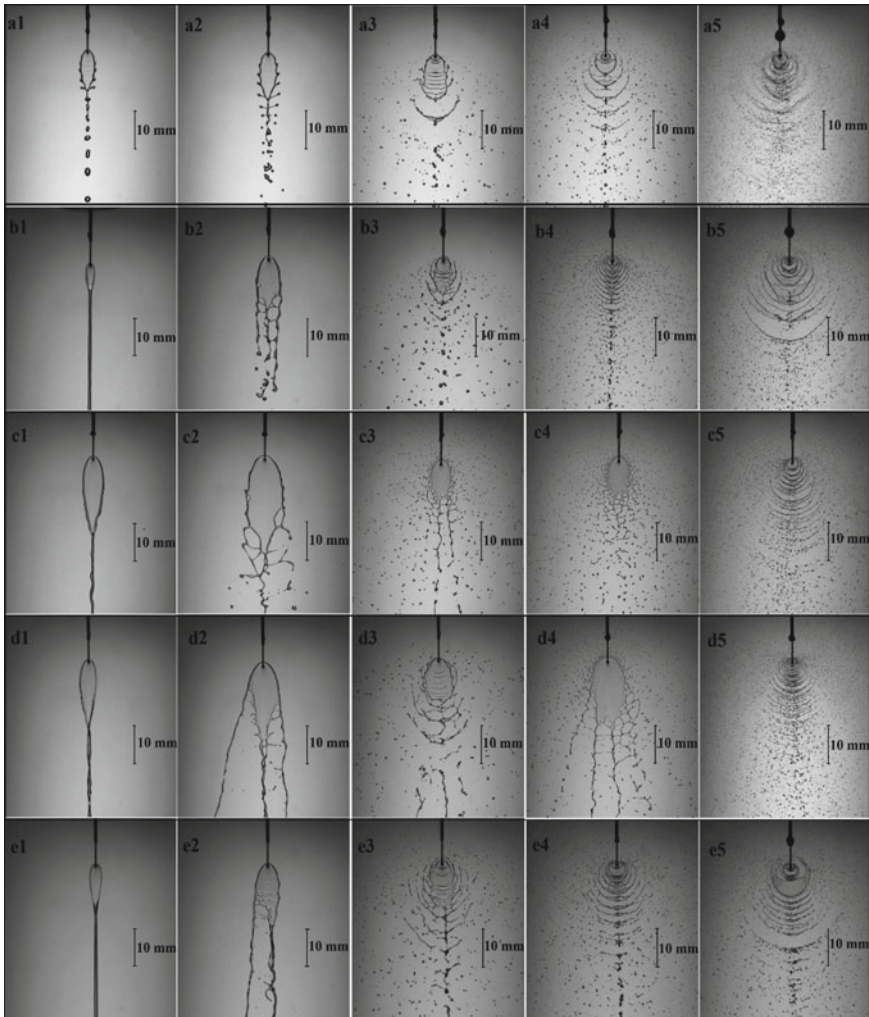
Fig. 4 Sheet break-up length and width representation for five gel concentrations. **a** 0.10 wt%, **b** 0.15 wt%, **c** 0.20 wt%, **d** 0.25 wt%, and **e** 0.30 wt%

The fluid elements are emerging from the impingement point spread in all directions for low jet velocities, as visible from Fig. 4. The vertical momentum of the liquid elements stretches the sheet a little above the impingement point. Note that sheet length is measured from the impingement point only (Fig. 4a1–a5). The liquid elements moving in the vertical direction above the impingement point in the sheet slowly lose their momentum and reach the rim of the sheet. These fluid elements then travel through the rim downwards and join other liquid elements that have lost momentum and continue to flow downward.

Any disruption in the jets is visible immediately on the rim. The horizontal component of velocity will slowly decay for fluid elements in the sheet. Only downward momentum persists, thus forming the sheet shape.

As jet velocity increases, the momentum of liquid elements also increases, resulting in the opening up of the bottom of the sheet. The fluid elements traveling in the rim have higher velocity, and this velocity helps them separate them from the hold of the liquid sheet. The sheet thickness near the rim must be less compared to other parts of the sheet. For higher concentration gels, the rim is seen to separate from the sheet without disintegration. Figure 4b2 shows the formation of perforations in the lower portion of the sheet. These perforations contain thin rims also.

Further increase in jet velocity is marked by a gain in momentum of fluid elements, which breaks out of the rim and spreads in the plane as droplets of various sizes. In Fig. 4, column three represents droplets emerging out from the sheet, but mostly below the impingement point. Images of higher viscosity gels look different from their lower concentration counterparts in the shape and size of liquid elements disintegrating from the sheet. While low-concentration gels form more droplets, the higher concentration ones mostly move out as ligaments.

For a higher concentration of gels shown, sheet break-up is mostly observed due to the sheet's tearing at the lower portion of the sheet. The multiple perforations formed in the sheet make it like a Web structure and are further stretched to form ligaments as they move away from the impingement point. This type of break-up is visible for cases b2–b3, c2–c4, d2–d4, and e2–e3. For 0.10 wt% gel, this mode is not visible under the ranges of jet velocities measured. One distinctive spray pattern for 0.10 wt% gel is that it behaves like water or a Newtonian fluid. It is because of low-viscosity value and high-surface tension similar to water.

Formation of waves originating from impingement point is visible for 0.10 wt% cases. These disturbances eventually cause the sheet to flap and disintegrate into droplets. As injection pressure increases, these disturbances are increasing, and it is seen that sheet dimensions are minimal and the bulk of fluid coming out of the orifices is moving away in waves after impingement. Frame a5 indicates a lot of atomization activity without any visible ligament formation. For gels of higher concentrations, especially from 0.20 wt% and above, wave-induced sheet break-ups are only visible at higher injection pressures (see Fig. 4c5, d5 and e5). The viscosity shear rate trend shows that the viscosity is attaining a value near to that of water at high shear rates. The shear rate achieved by the fluid is higher for higher injection pressures, and viscosity is reduced; this helps the formation of unstable wave generation at the impingement point.

Within each plot, break-up due to waves and perforations in the sheet are accommodated by giving red color boxes for wave-induced break-up and magenta for perforations induced break-up. For 0.10 wt%, gel wave-induced sheet break-up is prominent for a range of jet velocities studied. At low jet velocities (Fig. 4, column 1), sheet does not show break-up and continues to fall like a thread. As gel concentration increases, the lower portion of sheet has a higher tendency to form a single cylindrical (line) like flow structure. For low-viscosity gels like 0.10 wt%, the threads are visibly disintegrating into drops. In Fig. 5, a sheet break-up length and width are found to decrease initially and then increase. From frames, it was observed that due to increased occurrence of waves at higher jet velocity, the sheet got unstable, and as velocity further increased, more waves are created, and adjacent waves are found to overlap each other and a higher sheet dimension was observed.

For 0.15 wt% gel, wave-induced break-up cases show an initial increase in sheet dimension and then decreases for an increase in Reynolds number. For perforations induced break-up, the sheet length is found to decrease for an increase in Reynolds number. Sheet width for both break-up modes is approximately constant. For 0.20 wt% gel, perforations-induced break-up is found first to increase and then decrease for increasing Reynolds number.

For wave-induced break-up, the sheet dimensions decreased for an increase in Reynolds number. For 0.25 and 0.30 wt% gels, increase in Reynolds number causes reduction in sheet break-up length, but a slight increase in sheet width. Von Kampen et al. (2003) obtained a reduction sheet dimension for an increase in Reynolds number. This study conducted did not go to higher Reynolds number ranges to compare the results. For an increase in gel concentration, the drop velocity increase is observed for drops originating from the sheet's lower portion.

3.4 Droplet Profile and Velocity

From the edges of the sheet (see Fig. 4a2), small protrusions can be seen forming, trying to disrupt the sheet equilibrium. Depending on the jet velocity, the droplets attain velocities and follow particular trajectories. Figure 7 shows trajectories of a few liquid droplets for three gel concentrations for two different jet velocities. A set of 15–20 continuous frames is selected to trace three different droplets originating from the sheets of three different locations. Each droplet taken was considerably far from each other. Drop velocities are an average of all instances taken. Droplets originating from the top side of the sheet are having a higher horizontal velocity component. As jet velocity increases, the droplets are trying to move horizontally.

The velocity of droplets measured from these frames is presented in Fig. 7. As jet velocities increase, the droplet velocities also increase. It is observed that droplets originating from lower portion of the sheet have higher velocities than the droplets originating from the upper portion. For higher jet velocities, the increase in droplet velocity as we move down the sheet is also higher than the low jet velocity case. Waves starting to form from the impingement point are seen to slowly move in the
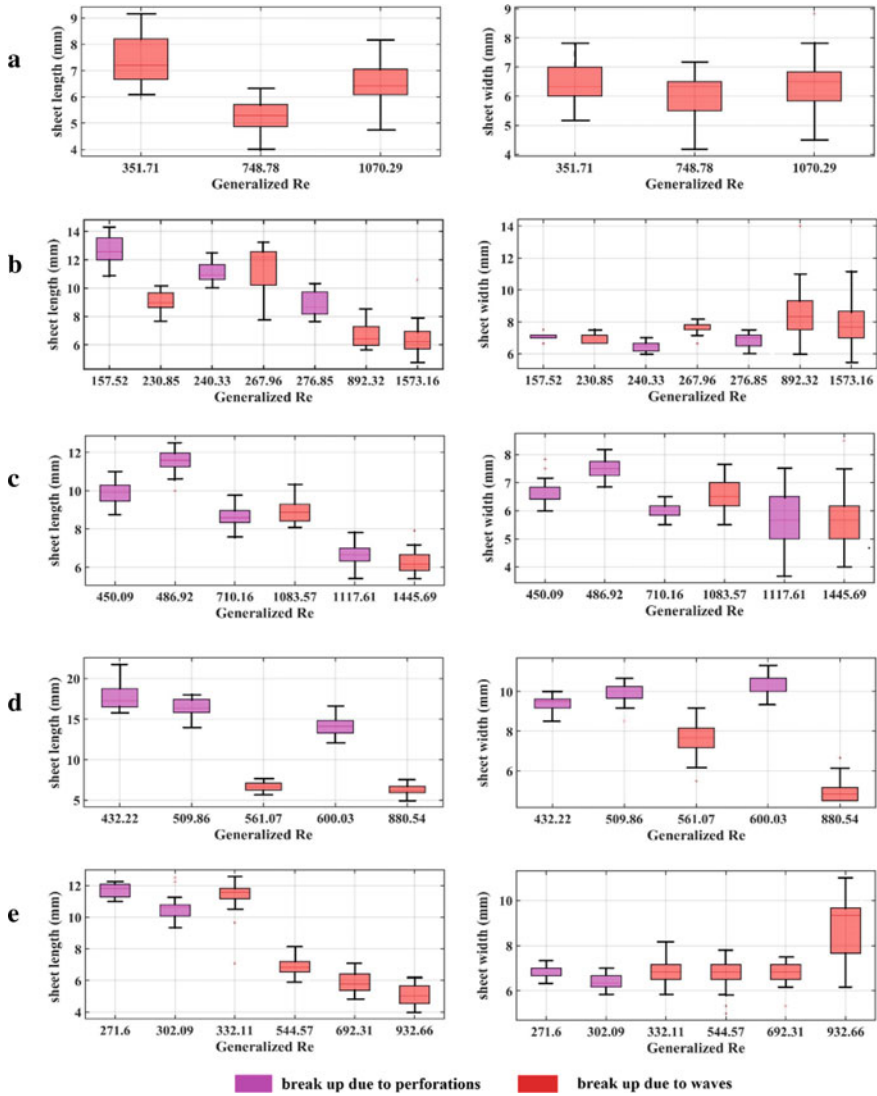
Fig. 5 Sheet break-up length versus generalized Reynolds number. Red color represents sheet break-up due to waves originating from impingement point and Magenta color represents sheet break-up due to perforations. X-axes and Y-axes represent sheet dimension in millimeter and generalized Reynolds number, respectively. **a** 0.10 wt%, **b** 0.15 wt%, **c** 0.20 wt%, **d** 0.25 wt%, and **e** 0.30 wt%
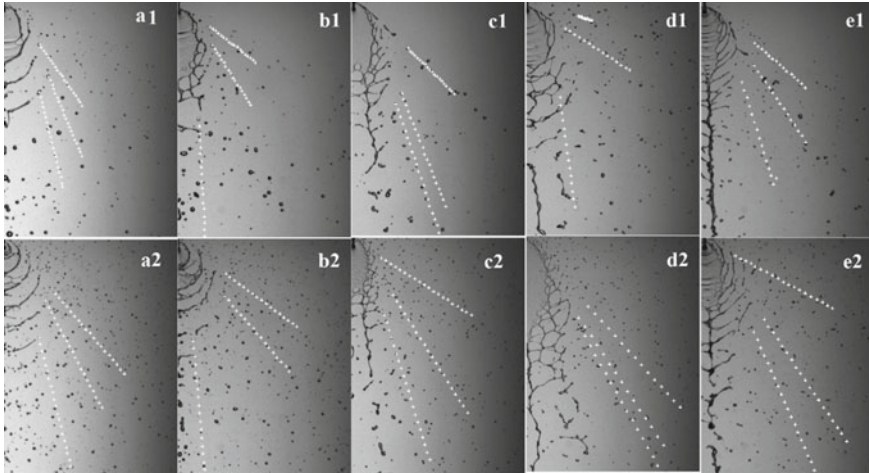
Fig. 6 Droplet trajectory followed for consecutive frames. **a1** and **a2** 0.10 wt%, and jet velocities 8.33 and 13.65 m/s. **b1** and **b2** 0.15 wt%, and jet velocities 7.02 and 9.94 m/s. **c1** and **c2** 0.30 wt%, and jet velocities 8.91 and 9.43 m/s. In each figure, trajectories of three different droplets are shown as white cross

form of an arc and the stretches to gain a horizontal shape and during this propagation, liquid droplets are thrown out from the ends. When these droplets are thrown before complete stretching, the velocity of droplets is found to be less. This occurs from waves near the impingement point. When waves stretch of in the middle of the sheet, the droplets emerging from its ends travel at a higher velocity. And liquid droplets found further downstream travel at an even higher velocity. The velocity of each droplet is observed to be constant for the displacement measured. For higher jet velocities, twenty number of instances were not obtained as the droplets move fast. In Fig. 6, one portion of the impinging jets is shown; the other is symmetric for most cases. As only three droplets are studied for each frame, a complete trajectory for droplets is not obtained and all locations in the sheet where droplet formation takes place are also not shown. For high concentration gels, the size of the droplets was not always spherical. An elliptical shape is more prominent.

4 Conclusions

Impinging jet atomization study of Carbopol gel is conducted experimentally. The focus was on sheet formation, disintegration mechanism for a range of Reynolds number and droplet velocity distribution for different jet velocities. As Reynolds number increases, sheet break-up lengths for perforations-induced break-up are
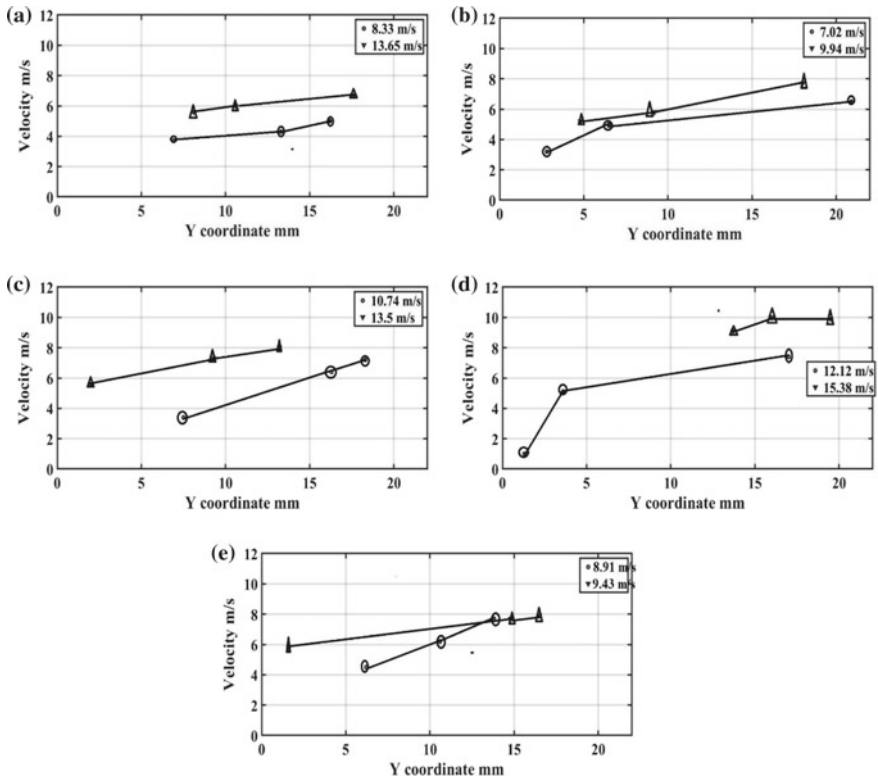
Fig. 7 Droplet velocity and drop origin location are represented for five gel concentrations. **a** 0.10 wt%, **b** 0.15 wt%, **c** 0.20 wt%, **d** 0.25 wt%, and **e** 0.30 wt%. For each case, drop velocity for two jet velocities is marked (the corresponding jet velocities are shown in legend)

found to decrease for 0.15–0.30 wt%. For higher Reynolds number, sheet break-up length for wave-induced break-up also reduced. Droplet velocity increases as we go down the sheet length. The droplet velocities are also found to be stable.

References

1. Heidmann MF, Priem RJ, Humphrey JC (1957) A study of sprays formed by two impinging jets. NACA technical note 3835
2. Anderson WE, Ryan HM, Pal S, Santoro RJ (1963) Fundamental studies of impinging liquid jets. AIAA, 1992, pp 92–0458. Dombrowski N, Hooper PC (1963) A study of the sprays formed by impinging jets in laminar and turbulent flow. J Fluid Mech 18(3):392–400
3. Ibrahim E, Przekwas A (1991) Impinging jets atomization. Phys Fluids A 3(12):2981–2987
4. Lai W-H, Huang T-H, Jiang T-L, Huang W (2005) Effects of fluid properties on the characteristics of impinging-jet sprays. Atom Sprays 15(4)
5. Green J, Rapp D, Roncace J (1991) Flow visualization of a rocket injector spray using gelled propellant simulants. In: 27th joint propulsion conference, pp 2198
6. Chojnacki K, Feikema D (1994) Atomization studies of gelled liquids. In: 30th joint propulsion conference and exhibit, 1994, p 2773
7. Jayaprakash N, Chakravarthy SR (2003) Impingement atomization of gel fuels. AIAA 316:2003
8. Kim J-Y, Song J-Y, Lee E-J, Park S-K (2003) Rheological properties and microstructures of carbopol gel network system. Colloid Polym Sci 281(7):614–623
9. Von Kampen J, Alberio F, Ciezki HK (2007) Spray and combustion characteristics of aluminized gelled fuels with an impinging jet injector. Aerosp Sci Technol 11(1):77–83
10. Ciezki H, Tiedt T, Von Kampen J, Bartels N (2005) Atomization behavior of Newtonian fluids with an impinging jet injector in dependence upon Reynolds and weber numbers. In: 41st AIAA/ASME/SAE/ASEE joint propulsion conference & exhibit, 2005, p 4477
11. Lee I, Koo J (2010) Break-up characteristics of gelled propellant simulants with various gelling agent contents. J Therm Sci 19(6):545–552
12. Fakhri S, Lee JG, Yetter R (2009) Atomization and spray characteristics of gelled-propellant simulants formed by two impinging jets. In: 45th AIAA/ ASME/SAE/ASEE joint propulsion conference & exhibit, 2009, p 5241
13. Baek G, Kim C (2011) Rheological properties of carbopol containing nanoparticles. J Rheol 55(2):313–330
14. Madlener K, Ciezki HK (2012) Estimation of flow properties of gelled fuels with regard to propulsion systems. J Propul Power 28(1):113–121
15. Baek G, Kim S, Han J, Kim C (2011) Atomization characteristics of impinging jets of gel material containing nanoparticles. J Nonnewton Fluid Mech 166(21–22):1272–1285
16. Yang L-J, Fu Q-F, Qu Y-Y, Gu B, Zhang M-Z (2012) Break-up of a power-law liquid sheet formed by an impinging jet injector. Int J Multiph Flow 39:37–44
17. Ma Y-C, Bai F-Q, Chang Q, Yi J-M, Jiao K, Du Q (2015) An experimental study on the atomization characteristics of impinging jets of power law fluid. J Nonnewton Fluid Mech 217:49–57
18. Jejurkar SY, Yadav G, Mishra D (2018) Characterization of impinging jet sprays of gelled propellants loaded with nanoparticles in the impact wave regime. Fuel 228:10–22
19. Jejurkar SY, Yadav G, Mishra D (2018) Visualizations of sheet break-up of non-Newtonian gels loaded with nanoparticles. Int J Multiph Flow 100:57–76